Electronic Supporting Information

Tuning the Langasite, $La_3SbZn_3Si_2O_{14}$ Towards White Light Emission: Synthesis, Structure, SHG and Photoluminescence Studies

Anupam Bhim, Ashutosh Mohanty and Srinivasan Natarajan*[a]

[a]*Framework Solids Laboratory, Solid State and Structural Chemistry Unit, Indian Institute of Science, Bangalore – 560012, India*.

E-mail: snatarajan@iisc.ac.in

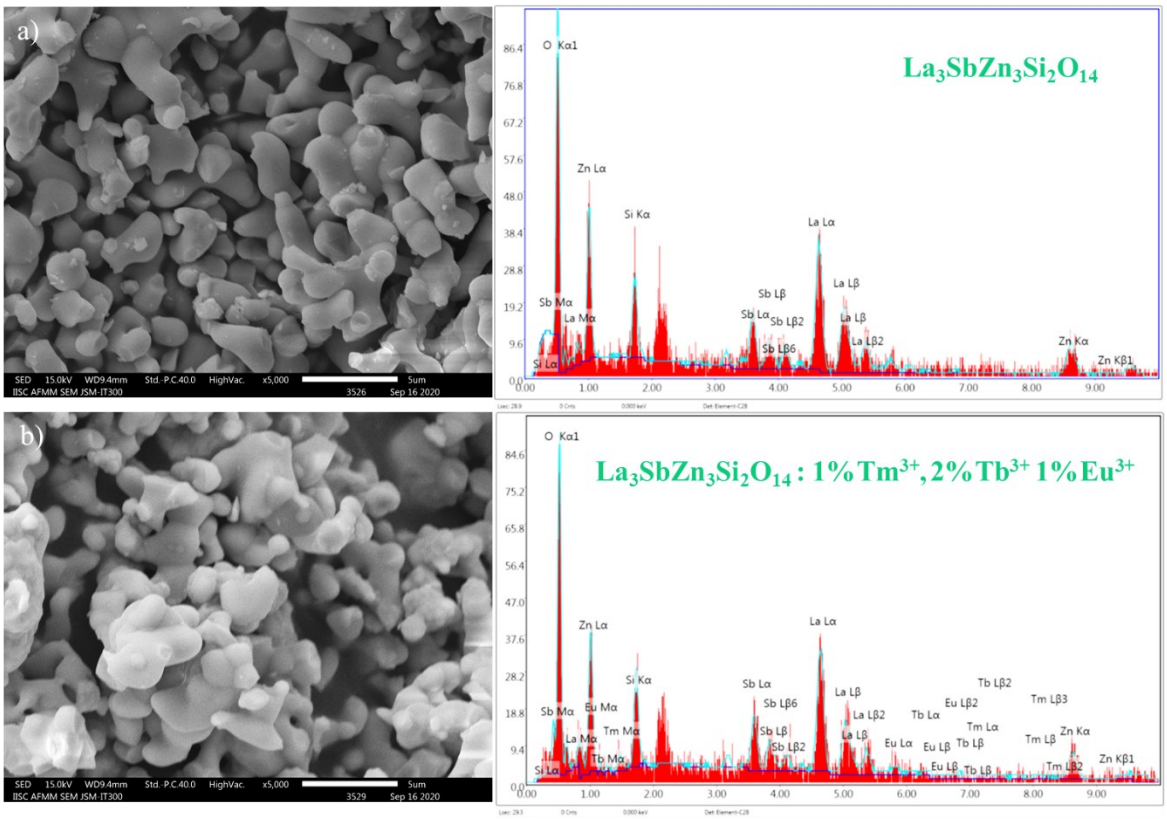

Figure S1. SEM image and corresponding EDX spectrum of (a) $La_3SbZn_3Si_2O_{14}$ and rare-earth doped $La_3SbZn_3Si_2O_{14}$.

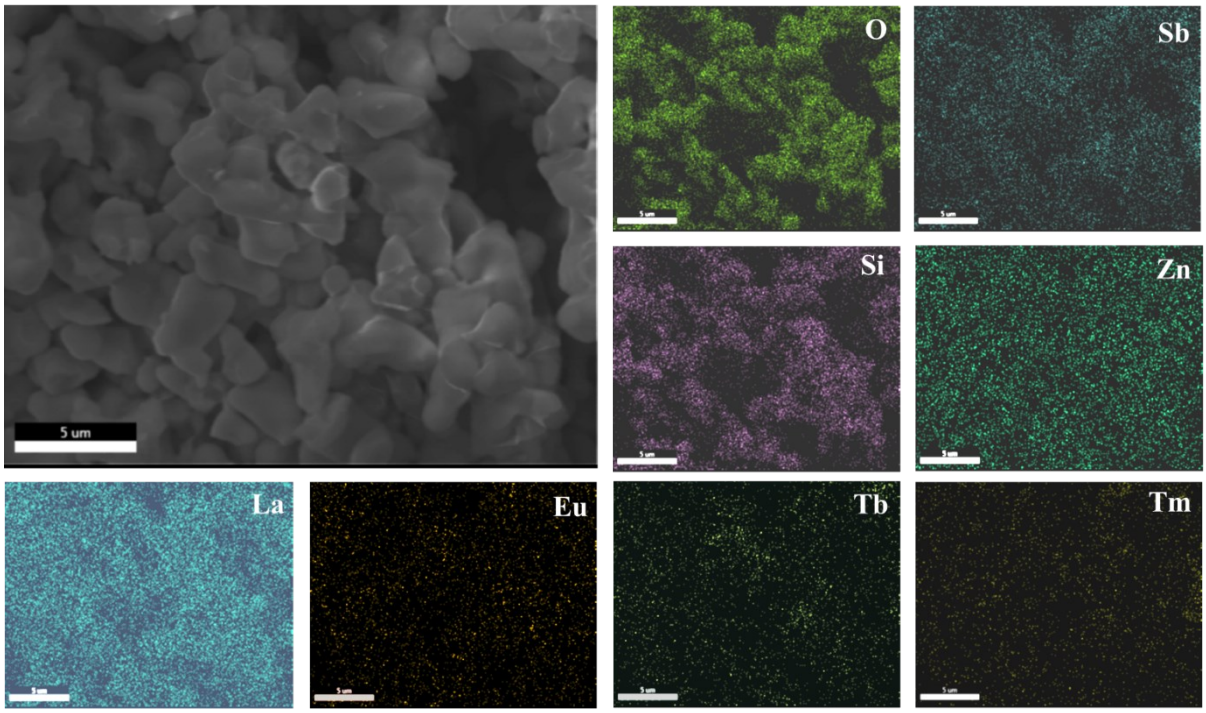

Figure S2. SEM-EDX elemental mapping for rare-earth doped $La_3SbZn_3Si_2O_{14}$ (1% Tm^{3+}, 2% Tb^{3+}, 1% Eu^{3+})

Table S1. Crystallographic data for $La_3SbZn_3Si_2O_{14}$ with trigonal structure.

Atom	Site	x	y	z	U_{iso}(Å^2)	Occupancy
La	*3e*	0.440468	0.0	0.0	0.015(2)	1.0
Sb	*1a*	0.0	0.0	0.0	0.011(2)	1.0
Zn	*3f*	0.750358	0.0	0.5	0.014(2)	1.0
Si	*2d*	0.333300	0.666700	0.490313	0.017(2)	1.0
O1	*2d*	0.333300	0.666700	0.785414	0.026(2)	1.0
O2	*6g*	0.492258	0.299794	0.634513	0.025(2)	0.667
O2	*6g*	0.492258	0.299794	0.634513	0.025(2)	0.333
O3	*6g*	0.223420	0.102585	0.236710	0.035(1)	1.0

Space group *P*321: $a = b = 8.219(2)$ Å, $c = 5.064(4)$ Å, $\alpha = \beta = 90°$, $\gamma = 120°$;

Reliability Factors: $R_p = 11.70\%$, $R_{wp} = 12.62\%$, $\chi^2 = 18.23$

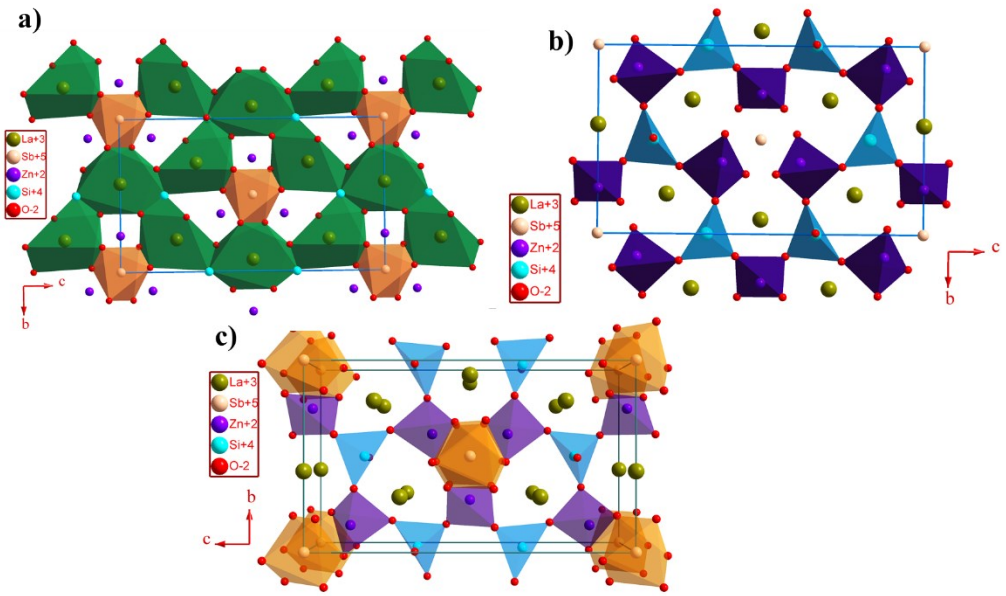

Figure S3. a) The polyhedral layer consisting of SbO_6 octahedra and two types of La polyhedra, b) The ZnO_4 and SiO_4 tetrahedra are corner shared via oxygen atoms, c) Projection of the $La_3SbZn_3Si_2O_{14}$ crystal structure upon the xz plane.

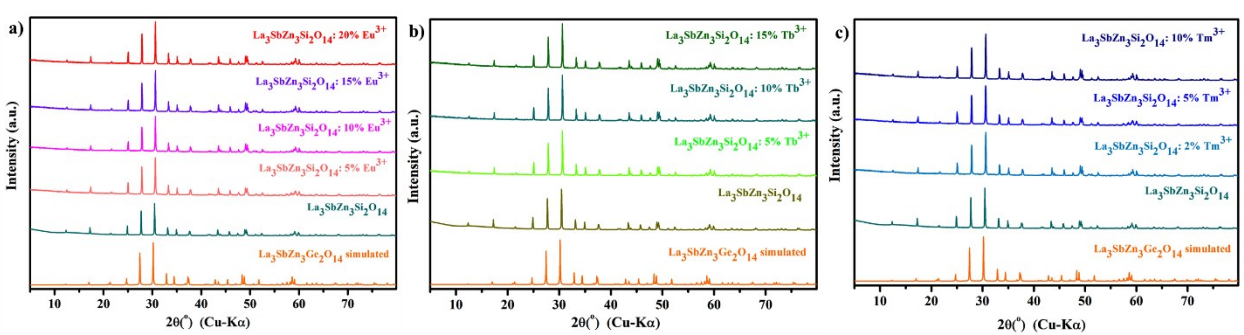

Figure S4. PXRD patterns of the rare earth doped $La_{3-x}M_xSbZn_3Si_2O_{14}$, ($0< x \leq 0.6$) for M = Eu, ($0< x \leq 0.5$) for M = Tb and ($0< x \leq 0.3$) for M = Tm compounds.

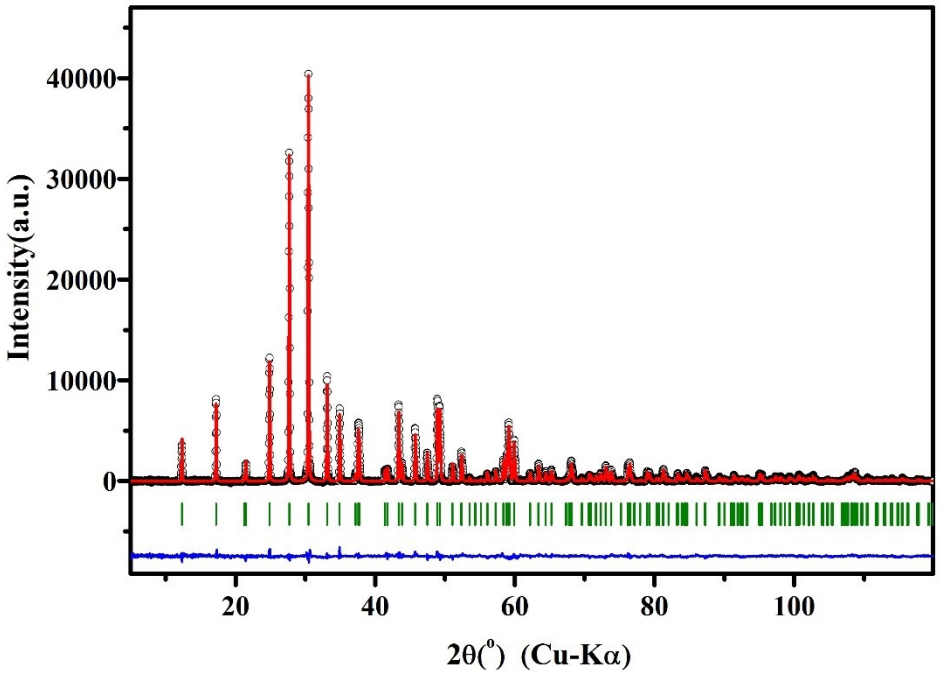

Figure S5. Rietveld refinement of rare-earth doped $La_3SbZn_3Si_2O_{14}$ (1% Tm^{3+}, 2% Tb^{3+} and 1 % Eu^{3+}) from the PXRD data. The observed (O), calculated (red line), and difference (bottom blue line) profiles are shown. The vertical bars (|) indicate Bragg reflections.

Table S2. Crystallographic data for rare-earth doped $La_3SbZn_3Si_2O_{14}$ (1% Tm^{3+}, 2% Tb^{3+} and 1 % Eu^{3+})

Atom	Site	x	y	z	U_{iso}(Å^2)	Occupancy
La1/Tm1/Tb1/Eu1	*2a*	0.0	0.436(2)	0.0	0.022(2)	0.98/0.005/0.01/0.005
La2/Tm2/Tb2/Eu2	*4c*	-0.002(2)	0.286(4)	0.287(1)	0.020(4)	0.98/0.005/0.01/0.005
Sb	*2a*	0.0	0.0	0.0	0.021(1)	1.0
Zn1	*2a*	0.5	0.744	0.0	0.030(5)	1.0
Zn2	*4c*	0.493(1)	0.121(2)	0.121(3)	0.008(2)	1.0

Si	*4c*	0.457(4)	0.514(2)	0.167(4)	0.024(6)	1.0
O1	*4c*	0.745(7)	0.464(1)	0.168(2)	0.027(2)	1.0
O2	*4c*	0.679(1)	0.857(4)	0.370(5)	0.011(2)	1.0
O3	*4c*	0.719(4)	0.135(2)	0.421(2)	0.038(3)	1.0
O4	*4c*	0.604(2)	0.141(3)	0.264(1)	0.076(1)	1.0
O5	*4c*	0.228(4)	0.978(2)	0.112(3)	0.062(5)	1.0
O6	*4c*	0.205(1)	0.342(2)	0.426(4)	0.007(2)	1.0
O7	*4c*	0.213(4)	0.688(6)	0.450(2)	0.008(4)	1.0

Space group *A*121: a = 5.127(2) Å, b = 8.237(5) Å, c = 14.284(3) Å, $\alpha = \gamma = 90°$, β =90.07°;

Reliability Factors: R_p = 3.48%, R_{wp} = 4.23%, χ^2 = 4.86;

Bond Lengths (Å): Zn–O = 1.959 (average), Sb–O = 1.996(1), Si–O = 1.579(2), La/Tm/Tb/Eu–O = 2.561 (average)

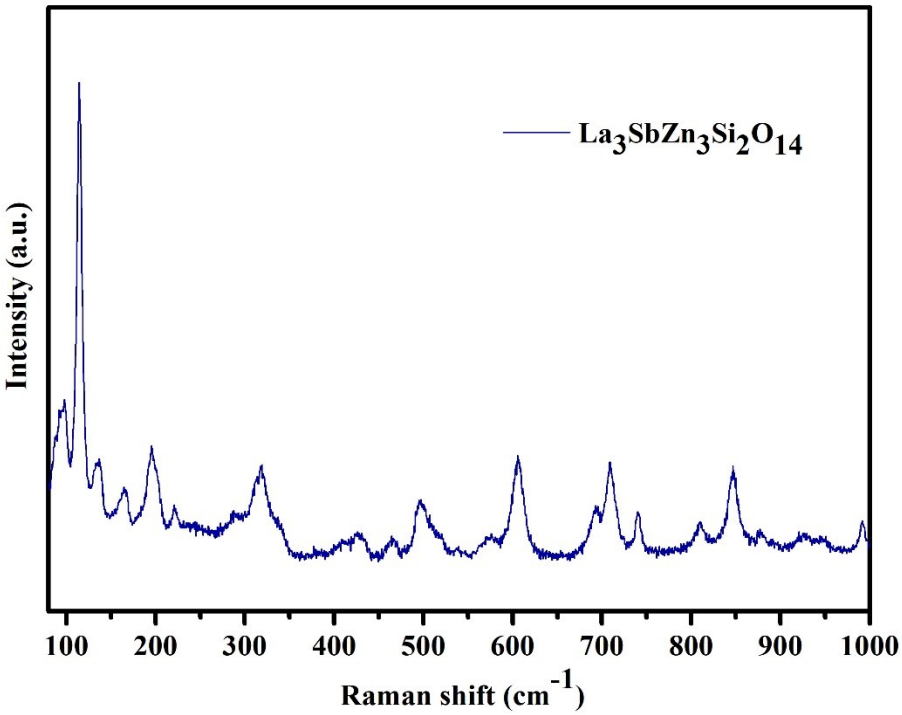

Figure S6. Raman spectra of $La_3SbZn_3Si_2O_{14}$ at room temperature.

Table S3. SHG Responses, for the prepared compounds

Compound	SHG at 1064 nm (×KDP)
$La_3SbZn_3Si_2O_{14}$	3.6
$La_3SbZn_3Si_2O_{14}$ (RE doped)	3.4

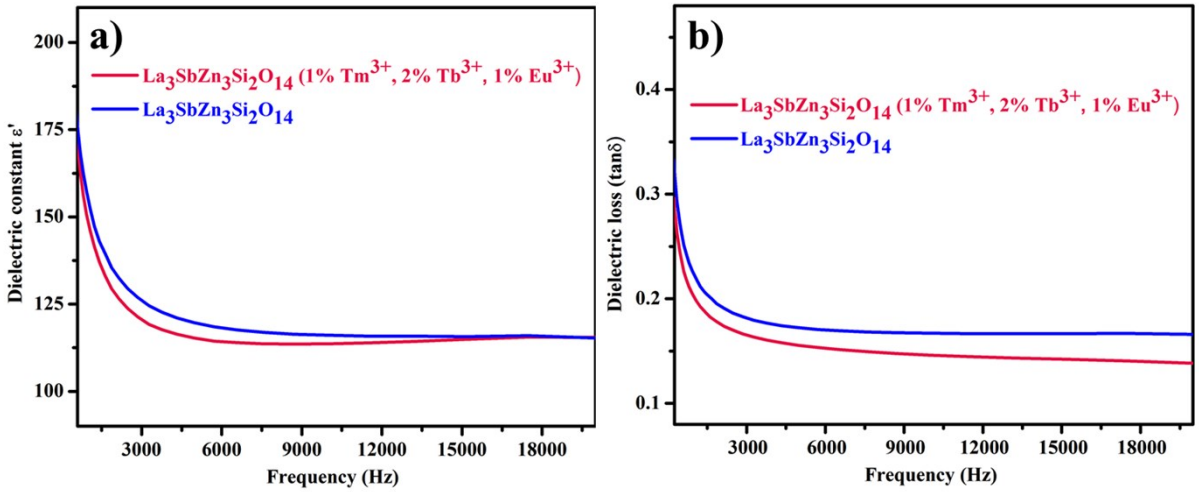

Figure S7. (a)The dielectric constant and (b) dielectric loss versus frequency plots for the Langasite compounds at room temperature.

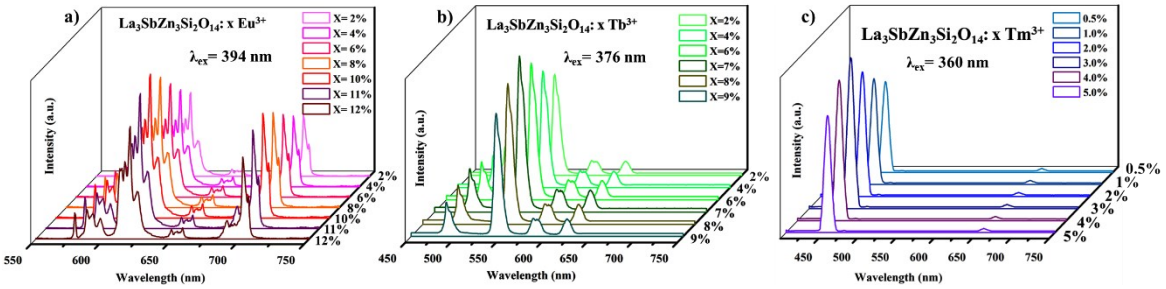

Figure S8. The variation of PL intensity as a function of the Eu^{3+}/Tb^{3+}/Tm^{3+} doping concentration.

Table S4. CIE chromaticity coordinates for $La_3SbZn_3Si_2O_{14}$ doped with 3% Tm^{3+}, 7% Tb^{3+}, and 10% Eu^{3+} samples

Compound	x	y
$La_3SbZn_3Si_2O_{14}$: 3% Tm^{3+}	0.14	0.10
$La_3SbZn_3Si_2O_{14}$: 7% Tb^{3+}	0.24	0.66
$La_3SbZn_3Si_2O_{14}$: 10% Eu^{3+}	0.62	0.34

Table S5. Comparison of the literature reported LED materials with the present Langasite host

Phosphor	Excitation Wavelength (nm)	Chromaticity coordinates (x,y)	CCT(K)	Quantum efficiency (%)	Ref.
YPO_4: (2%) Eu^{3+}, (5%) Tb^{3+}, (2%) Tm^{3+}	362	(0.315,0.273)	6995	-	1
$CaMoO_4$: (4%) Eu^{3+}, (4%) Tb^{3+}, (4%) Tm^{3+}	350	(0.340,0.330)	5095	-	2
$LiGd(WO_4)_2$: (2%) Eu^{3+}, (4%) Tb^{3+}, (3%) Tm^{3+}	360	(0.343,0.327)	4980	9	3
$K_3La(PO_4)_2$: (7%) Eu^{3+}, (30%) Tb^{3+}, (10%) Tm^{3+}	358	(0.366,0.333)	4072	38.2	4
$NaYGeO_4$: (12%) Eu^{3+}, (7%) Tb^{3+}, (3%) Tm^{3+}	369	(0.352,0.376)	4842	40.2	5
$Na_2Y_2B_2O_7$: (0.5%) Eu^{3+}, (60%) Tb^{3+}, (0.5%) Ce^{3+}	365	(0.403,0.487)	4095	77	6
$NaGd(WO_4)_2$: (4%) Eu^{3+}, (3%) Dy^{3+}, (1%) Tm^{3+}	365	(0.364,0.322)	4040	-	7
$Ca_3Bi(PO_4)_3$: (9%) Eu^{3+}, (10%) Tb^{3+}, (4%) Tm^{3+}	360	(0.338,0.329)	5282	-	8
$La_3SbZn_3Si_2O_{14}$: (1%) Eu^{3+}, (2%) Tb^{3+}, (1%) Tm^{3+}	360	(0.337,0.348)	5309	16	This work

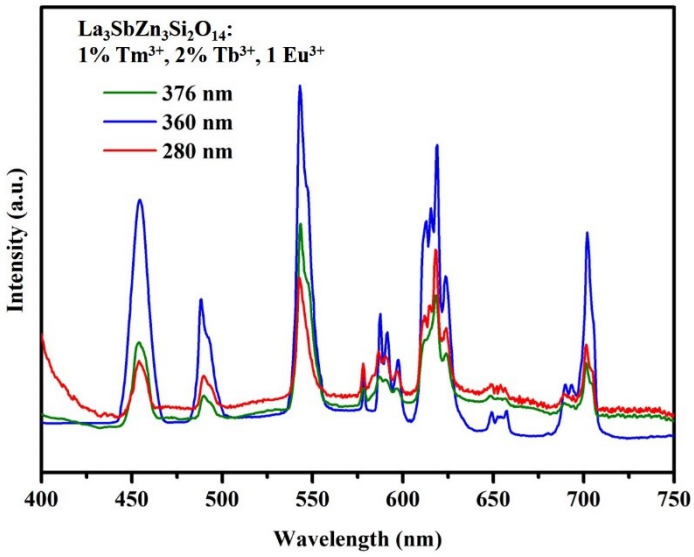

Figure S9. The compound, $La_3SbZn_3Si_2O_{14}$ (1% Tm^{3+}, 2% Tb^{3+} and 1 % Eu^{3+}) excited at different wavelength.

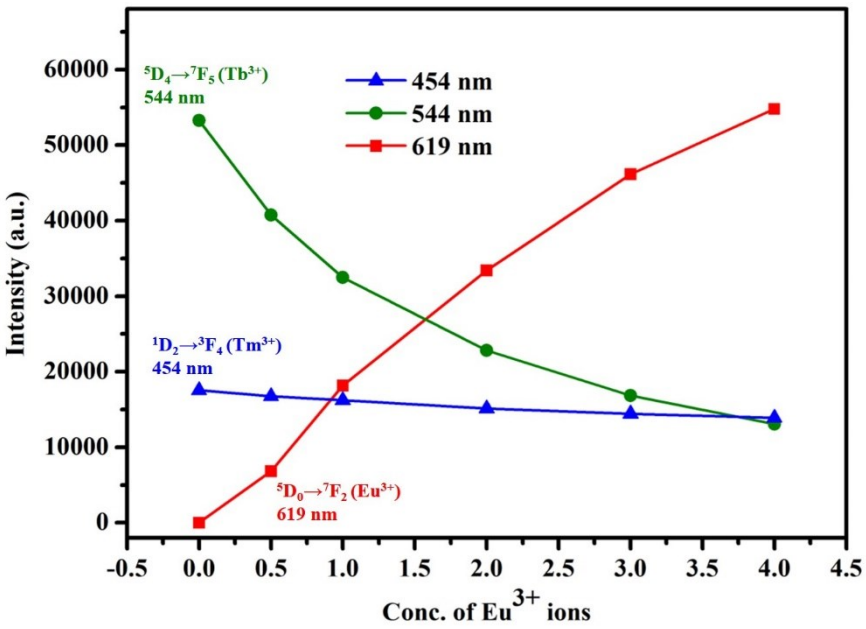

Figure S10. Variation of emission intensities at 454 nm ($^1D_2 \rightarrow {}^3F_4$), 544 nm ($^5D_4 \rightarrow {}^7F_5$), and 619 nm ($^5D_0 \rightarrow {}^7F_2$) vs. Eu^{3+} concentrations in $La_3SbZn_3Si_2O_{14}$: 1% Tm^{3+}, 2% Tb^{3+}, *x*% Eu^{3+} (*x* = 0, 0.5, 1.0, 2.0, 3.0, 4.0) compounds under 360 nm excitation.

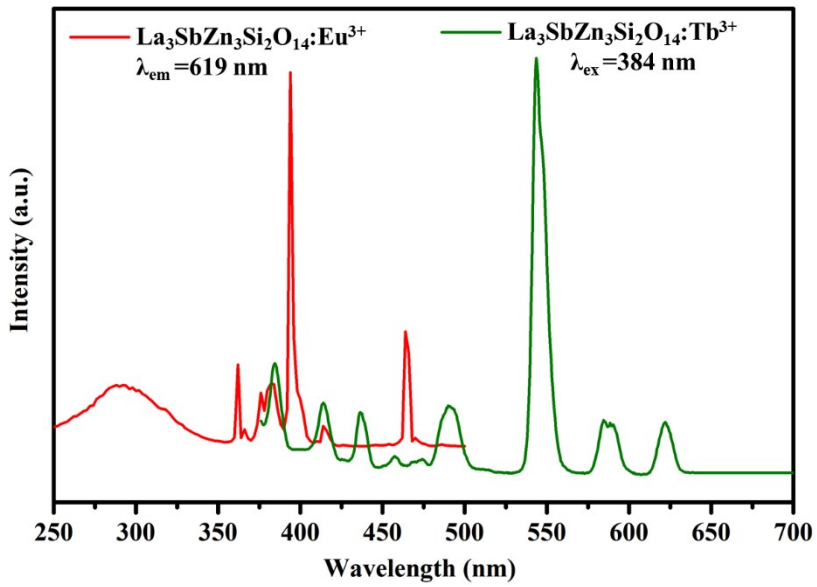

Figure S11. The spectral overlap between the PLE spectrum of $La_3SbZn_3Si_2O_{14}$: Eu^{3+} and PLE spectrum of $La_3SbZn_3Si_2O_{14}$: Tb^{3+} phosphors.

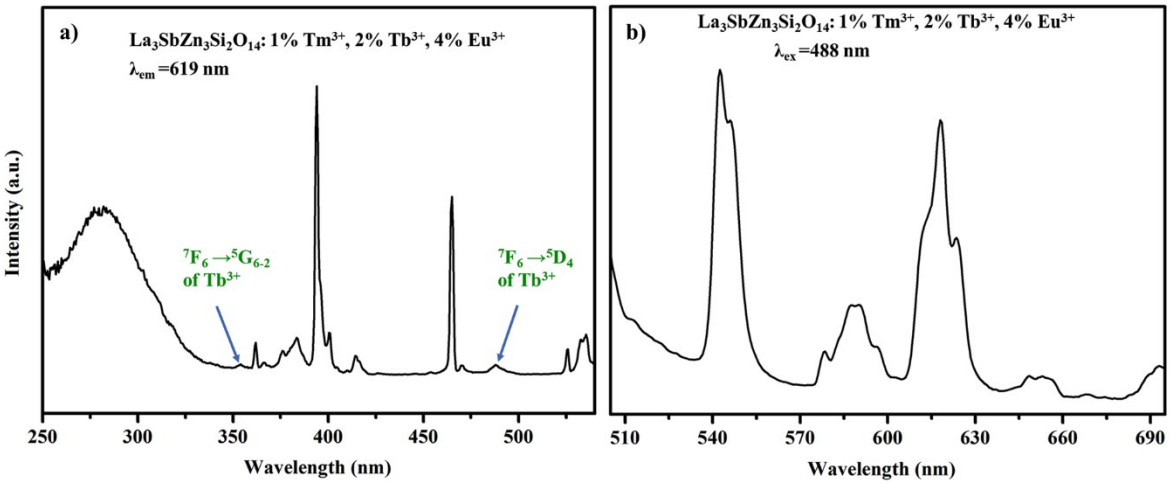

Figure S12. a) The excitation spectrum of $La_3SbZn_3Si_2O_{14}$:1% Tm^{3+}, 2% Tb^{3+}, 4% Eu^{3+} sample monitored at 619 nm; b) The emission spectrum of the sample at the excitation of 488nm.

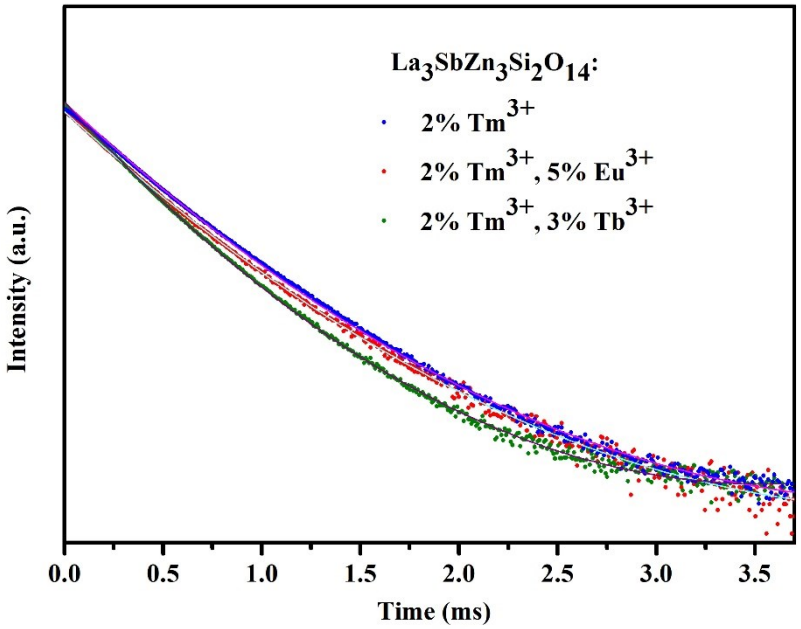

Figure S13. The decay curves for the luminescence of Tm^{3+} ions in $La_3SbZn_3Si_2O_{14}$: 2% Tm^{3+}; 2% Tm^{3+}, 5% Eu^{3+}; 2% Tm^{3+}, 3% Tb^{3+} samples (excited at 360 nm, monitored at 454 nm).

References

1. a) Z. Yahiaoui, M.A. Hassairi, M. Dammak, E. Cavalli, *J. Alloys Compd.,* 2018, **763**, 56–61.

2. R. L. Tranquilin, L. X. Lovisa, C. R. R. Almeida, C. A. Paskocimas, M. S. Li, M. C. Oliveira, L. Gracia, J. Andres, E. Longo, F. V. Motta and M. R. D. Bomio, *J. Phys. Chem. C,* 2019, **123**, 18536–18550.

3. Y. Zhang, W. T. Gong, J. J. Yu, Y. Lin and G. L. Ning, *RSC Adv*., 2015, **5**, 96272–96280.

4. X. Wu, W. Bai, O. Hai, Q. Ren, J. Zheng, Y. Ren, *Opt. Laser Technol.,* 2019, **115**, 176–185.

5. W. Zhao, X. Feng, B. Fan, *J. Mater. Sci.: Mater. Electron*, 2020, **31**, 14434–14442.

6. D. Wen and J. Shi, *Dalton Trans*., 2013, **42**, 16621–16629.

7. Y. Liu, G. Liu, J. Wang, X. Dong and W. Yu, *Inorg. Chem*., 2014, **53**, 11457–11466.

8. M. M. Jiao, N. Guo, W. Lu, Y. C. Jia, W. Z. Lv, Q. Zhao, B. Q. Shao and H. P. You, *Dalton Trans*., 2013, **42**, 12395–12402.